This article has been accepted for publication in a future issue of this journal, but has not been fully edited. Content may change prior to final publication. Citation information: DOI 10.1109/JIOT.2020.3024017, IEEE Internet of Things Journal

Dual-Band Store-and-Use System for RF Energy Harvesting with Off-the-Shelf DC/DC Converters

Fernando Moreno-Cruz, Víctor Toral-López, Marina Ramos Cuevas, José F. Salmerón, Almudena Rivadeneyra and Diego P. Morales

***Abstract*—RF energy harvesting (RFEH) has recently become part of the alternatives for powering wireless sensor networks. Our focus in this paper was to introduce a design, *MSwitch*, able to use off-the-shelf dc/dc converters for running a real and self-powered Internet of Things (IoT) application. *MSwitch* is an RF dual-band energy harvesting stage employing the store-and-use principle, that mixes efficiently and in a dynamic manner both inputs. We proved an increase on the performance with respect to the single band case and to the most successful approaches found in the literature, achieving about 10% better efficiency and around 35% lower minimum power levels. Besides, we carried out an analysis on the commercial dc/dc converters, characterizing them for ultra-low power conditions. Likewise, we analyzed the state-of-the-art rectification circuits and commercial Schottky diodes, searching the best performance under our RFEH conditions. Finally, we manufactured our designs as a complete system and demonstrated its operation with an IoT concrete application.**

***Index Terms*—Radio frequency energy harvesting (RFEH), dc/dc converters, wireless energy transmission (WET), dual-band, rectification, wireless sensor networks (WSN), Internet of Things (IoT), Schottky diode.**

I. Introduction

THE MASSIVE deployment of Internet of Things (IoT) within our society is an irrefutable reality. Everyday ordinary objects, vehicles, buildings, etc., are being merged with electronics as part of a wireless sensor network (WSN), needing an energy source. They will provide new perspectives to a wide range of areas like industry, healthcare, transportation, telemetry, home and city automation, energy conservation and security, among others.

The power and longevity demands of IoT devices vary broadly depending on the application, in view of their heterogeneous nature. They become a challenge when powering the nodes for a minimum time frame of weeks or months, even years, without compromising the quality of service. A common choice for their power source are non-rechargeable chemical batteries (e. g., lithium, deeply contaminant) [1]. However, for several use-cases are impracticable: in a large-scale deployment or when the device is hard to access, frequent battery replacement or recharge are infeasible by cause of the cost; or simply due to the power consumption and expected run-time. Furthermore, the environmental influence of the massive use of batteries, rechargeable and not, might be enormous and undoubtedly harmful [2], [3].

In this context appears energy harvesting (EH), as the process of capturing small amounts of diverse ambient energy, converting it into electricity and storing it. More particularly, radio frequency energy harvesting (RFEH) devices capture the energy present at the signal carriers in the far field region of ambient radiation. The frequencies of operation are between some kilohertzs and hundreds of gigahertzs [4], which later on are converted to dc.

RFEH can be also used as a wireless energy transmission (WET) technique. The difference is the use of a dedicated energy source that actively radiates. The received power is higher and reaches the requirements of more applications, since the power levels handled in harvesting are typically three orders of magnitude lower [5].

As most of the EH sources within the IoT world and their applications, RFEH may be categorized as "ultra-low power" (barely tens of microwatts) [6]. Currently there is a lack of dc/dc converters in the market for such low levels of power, being them considered for "low-power" conditions (range of milliwatts). This makes the use of EH techniques harder, since the converter stage, needed for getting a proper and stable voltage level, must be custom designed. For that reason, we have developed a battery-less dual-band system capable of harvesting RF energy while using off-the-shelf low-power dc/dc converters. The setup is based on the the store-and-use principle [7], by means of an intermediate stage formed by an innovative autonomous and dynamic switched capacitor design.

A. Related Work

Since Nikola Tesla originally proposed and demonstrated WET in the 1890's [8], the field has grown and matured finding its way to commercial applications [9]. Particularly during the last decade, WET has caught research attention in its two variants (harvesting and active transfer) and far from its hefty origins, the trend has been moved to WSN, where the main objective is the increase of the rectification and conversion efficiencies for low power [5].

The efficiency rapidly drops when the load impedance or the input power decrease ($<1\,\mathrm{M\Omega}$ and $<-10\,\mathrm{dBm}$), and so does the dc output voltage if not controlled [7]. RF-dc conversion efficiencies around 80% has been reported for input powers greater than $-10\,\mathrm{dBm}$, with an output load

Manuscript received April 20, 2020; accepted September 6, 2020.

F. Moreno-Cruz is with Infineon Technologies AG, Germany, e-mail: Fernando.MorenoCruz@infineon.com.

M. Ramos Cuevas is with the Technical University of Munich, Germany.

V. Toral, J.F. Salmerón, A. Rivadeneyra and D.P. Morales are with the Department of Electronics and Computer Technology, University of Granada, Spain, e-mail: (see http://electronica.ugr.es/index.php?sec=personal).

This article has been accepted for publication in a future issue of this journal, but has not been fully edited. Content may change prior to final publication. Citation information: DOI 10.1109/JIOT.2020.3024017, IEEE Internet of Things Journal

around $50\,\mathrm{k}\Omega$ at various microwave frequencies by Agrawal *et al.* [10]. With a 130 and $90\,\mathrm{nm}$ CMOS-based rectifiers, Oh and Wentzloff [11] and Stoopman *et al.* [12] respectively reached sensitivities of -32 and $-27\,\mathrm{dBm}$ both at $1\,\mathrm{V}$ output, although with a capacitive load impedance. Table I summarizes the best efficiencies and minimum RF sensitivities achieved in the literature and the most recent studies to the best of our knowledge. Powercast [9] in turn, presents a commercial power receiver with a minimum sensitivity of $-11.5\,\mathrm{dBm}$ at $1.8\,\mathrm{V}$ dc output for $915\,\mathrm{MHz}$ using an internal ad hoc boost converter.

For the rectification there are two main technologies implementing diode-based circuits: CMOS, that allows a lower minimum RF input power, and silicon Schottky barrier diodes, with normally better peak efficiency. Additionally, voltage multiplier or a simple diode structure are the most employed circuits [5]. For instance, Chouhan *et al.* [8] and Park *et al.* [17] present cascading schemes for the voltage multiplier fabricated in $0.18\,\mu\mathrm{m}$ CMOS and Schottky barrier technology respectively. Asl and Zarifi [18] also reports a 13 stages rectifier in $0.18\,\mu\mathrm{m}$ CMOS.

Most of the studies aim at a specific frequency channel, although multi-band is employed as well [19]. These designs target arrays composed of multiple antennas or, less frequently, broadband circuitry, focused on the matching network, as Khansalee *et al.* [20]. Piñuela *et al.* [14] builds rectennas and compares different array architectures, demonstrating the operation in a real scenario with a commercial voltage converter (BQ25504) and an LED as application. Donno *et al.* [21] and Liu and Sánchez-Sinencio [22] propose custom dc/dc converters, both charge pump designs and [22] with hill-climbing maximum power point tracking (MPPT).

The store-and-use principle is introduced by Singh *et al.* [7] with a tuned rectifier, achieving promising results in efficiency for low powers. [7] employs two power gates for controlling the energy flow to the load. The first one which runs the store-and-use procedure is not described, the second one achieved by a commercial converter (LTC3108).

B. Contribution

In this work, we propose a complete autonomous system for enabling and simplifying the use of RFEH in IoT nodes through an innovative design based on the store-and-use principle and using commercial dc/dc converters. Figure 1 shows the block diagram including the final application.

Two independent antennas capture the incident RF power at two different frequencies (dual-band), whose impedances are adapted to the rectifier stage by both matching networks. The dc power is now stored in two capacitors. The output of these capacitors to the converter stage is regulated by the logic of *MSwitch* depending on their voltage levels, being able even to completely isolate them. This mechanism enables their charging process in adverse power conditions, since the voltage level never collapses. The harvested energy enters the dc/dc converter, which finally maintains constant the output voltage for the application through a third storage capacitor.

The modularity of the system and versatility of *MSwitch* allow to change easily the frequency band or even to take advantage of its benefits for other EH techniques by only changing the energy input, being compatible with a broad range of power levels.

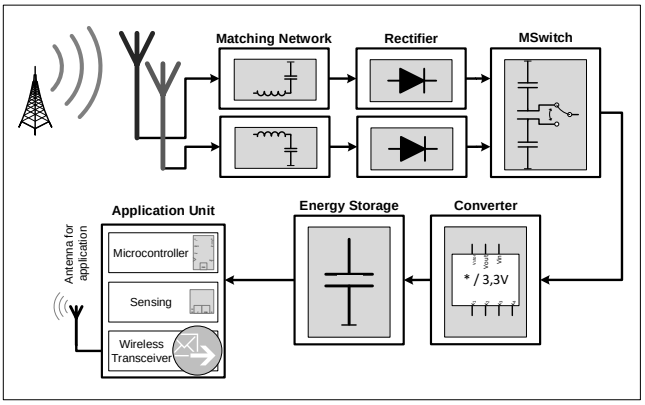

Fig. 1. Overview of whole system.

The main contributions of this paper are outlined as follows.

1) We present an innovative dual-band store-and-use auto-regulated and autonomous design for RFEH (or any other energy source), demonstrating an improvement to the state-of-the-art for its use with commercial dc/dc converters.
2) We analyze the best options of rectifier circuits and diodes, first with simulations and later in the laboratory under the expected power conditions.
3) In parallel, we perform a search among all commercially available dc/dc converters to date and analyze the most efficient ones with ultra-low power levels, taking them often out of the data-sheet characterization. The idea behind was to identify under which circumstances of low power and low voltage they can operate correctly and with which efficiency.
4) We characterize and develop the rest of the system needed stages, targeting an IoT application and manufacturing the best combination.
5) We demonstrate its operation with a model IoT application at the $949\,\mathrm{MHz}$ global system for mobile communications (GSM) band, formed by a $2.4\,\mathrm{GHz}$ transceiver and a temperature sensor.

For the detailed understanding, the model of the initial conditions is presented in Section II; in Section III, we describe the whole system and its operation. In Section IV, we analyze the performance achieved in every stage, focusing Section V on the whole system results and finally, Section VI, draws the main conclusions of this work.

II. System Model

In this section, we present the initial conditions found when diving into RFEH for WSN.

A. Electromagnetic Spectrum

The electromagnetic spectrum is regulated by allocating the different communication bands and, for safety and interference

This article has been accepted for publication in a future issue of this journal, but has not been fully edited. Content may change prior to final publication. Citation information: DOI 10.1109/JIOT.2020.3024017, IEEE Internet of Things Journal

TABLE I
PERFORMANCE COMPARISON OF STATE-OF-THE-ART CIRCUITS AND SYSTEMS FOUND IN THE LITERATURE

Related Work	Technology	Frequency	Minimum RF P_{in} @ Output Voltage	Conversion Efficiency @ RF P_{in}
Powercast 2110B [9]	-	915 MHz	−11.5 dBm @ 1.8 V	N. A.
Agrawal *et al.* [10]	HSMS-2852	900 MHz	−10 dBm @ 1.3 V	80% @ −10 dBm (60 kΩ)
Franciscatto *et al.* [13]	HSMS-2852	2.45 GHz	0 dBm @ 1.2 V	70.4% @ 0 dBm
Oh and Wentzloff [11]	130 nm CMOS	915 MHz	−32 dBm @ 1 V (cap. load)	N. A.
Stoopman *et al.* [12]	90 nm CMOS	886–915 MHz	−27 dBm @ 1 V (cap. load)	40% @ −17 dBm (1 MΩ)
Piñuela *et al.* [14]	SMS-7630	886–915 MHz	−25 dBm (converter)	40% (end-to-end, real GSM)
	+dual band		−29 dBm (converter)	15% (end-to-end, real GSM)
Nguyen *et al.* [15]	65 nm CMOS	950 MHz	−20 dBm @ 0.9 V	57% @ −10 dBm (10 kΩ)
Xu *et al.* [16]	65 nm CMOS	2.45 GHz	−17.1 dBm @ 0.4 V	48.3% @ −3 dBm (conv.)

reasons, limiting the emitting power. Several studies [23]–[25] assert that the present energy levels in city open-spaces reach $-30\,\mathrm{dBm}$ and even $-20\,\mathrm{dBm}$ at bands of high utilization, as the cellular network (GSM and its successors), TV broadcasting or wireless local networks; although the duty-cycle also varies.

For instance, a typical GSM base station in the $900\,\mathrm{MHz}$ band with a rating of $30\,\mathrm{W}$ and a $17\,\mathrm{dBi}$ antenna gain produces a theoretical power density of $600\,\mu\mathrm{m/m^2}$ at $500\,\mathrm{m}$, according to the Friis transmission equation [5]. Although the signals pathloss follows this equation, it is only valid in free space propagation and assuming direct line-of-sight, being normally received a lower level. Hence, the maximum received power with a standard monopole antenna of $2\,\mathrm{dBi}$ will be up to $8\,\mu\mathrm{W}$ ($-20\,\mathrm{dBm}$).

B. Energy Harvesting

Once the antenna captures the signal, a matching network is needed (maximum power transfer theorem) in order to maximize the power transmission to the rectifier and minimize the reflection coefficient.

Assuming a $50\,\Omega$ commercial antenna, the open-circuit voltage seen at the antenna of the example given above will be $20.5\,\mathrm{mV\,RMS}$. Accordingly, even with the voltage boosting of an ideal matching network at its resonant frequency, these levels do not suffice for reaching the turn-on threshold of present electronics at the rectifier. In addition, due to the high frequency of the bands we are dealing with, fast switching circuits are needed. For these reasons, Schottky diodes with a fast metal-semiconductor junction emerge as one of the only valid technologies.

For a proper application operation, the rectified voltage must be stable and at a specific level. A dc/dc converter runs this action, although with commercially available ones, we find several restrictions derived from the calculations made before: 1) too low voltage input, even though some converters can boost voltages as low as $20\,\mathrm{mV}$; 2) too low energy input, normally they can start their operation at around $50\,\mu\mathrm{W}$; and 3) too low input impedance, which drives the whole system to even lower voltage levels. Trying to solve these constrains with a custom design brings 4) higher price and effort. Therefore, an intermediate stage as the one presented in this paper appears as a promising solution.

Furthermore, the losses while storing the energy can be significantly adverse. Low leakage capacitors must be used (up to $0.5\,\mu\mathrm{A}$ at $3\,\mathrm{V}$) and in case of needing bigger capacitance (super-capacitors, up to $5\,\mu\mathrm{A}$ at $5.5\,\mathrm{V}$), special attention must be given to the storage voltage level in pursuance of the lowest leakage current, as well as to the time of storage.

C. Application Unit Requirements

An IoT application unit consists mainly of a microcontroller (μC), at least one sensor or actuator and a transceiver with an antenna. The target applications are those which do not require constant operation but a duty-cycled one, and which use ultra-low power radio-transceivers and sensors.

In this way, for a simple node measuring ambient temperature, humidity and air pressure and sending it to a gateway, the energy demand is around $1\,\mathrm{mJ}$ during the active mode (where the measurements and communication are done). In deep-sleep mode (where the batteries or capacitors are charged again) the consumption is close to null (less than $300\,\mathrm{nW}$ in some μCs) [4]. To sum up, the average power consumption for periods of, for example, $1\,\mathrm{h}$ would be around $600\,\mathrm{nW}$.

III. RFEH CIRCUIT DESIGN AND IMPLEMENTATION

During the design and implementation of the proposed system, we evaluated each stage independently with the evident dependencies at the interfaces (see Figure 1) and later on, we assembled them together, pursuing the best efficiency and lowest RF input power to start running the harvester. Before fabricating the final prototype, we carried out diverse simulations to prove our assumptions and improve the chosen circuits and components.

A. RF Bands, Antennas and Matching Network

We first examined the legal distribution of the spectrum in Europe from the electronic communications committee (ECC) [26] and followed the studies referred in Section II-A about its utilization. We concluded that the most convenient technologies to harvest from are the cellular network for outdoor use-cases (from GSM until 4G) and the Wi-Fi network for indoor. In any case, the modular design facilitates its exchange in a broad frequency range.

Due to the existence of several frequency bands within the cellular network, whose presence depends on the service providers and the base stations nearby, we performed a spectrum

This article has been accepted for publication in a future issue of this journal, but has not been fully edited. Content may change prior to final publication. Citation information: DOI 10.1109/JIOT.2020.3024017, IEEE Internet of Things Journal

measurement on our test environment to identify the most favorable bands. The scenario consists of an office area on the outskirts of Munich (Germany) of around $0.22\,\mathrm{km}^2$ from which $0.1\,\mathrm{km}^2$ is free space and the rest three-floors buildings. The measurements were made with a Keysight FieldFox Handheld N9917A spectrum analyzer. The most energetic frequencies found were $949\,\mathrm{MHz}$, corresponding with the 935–$960\,\mathrm{MHz}$ GSM band; $2159\,\mathrm{MHz}$, from the 2110–$2170\,\mathrm{MHz}$ international mobile telecommunications (IMT) band (i. e., 2G and 3G) and the $2.4\,\mathrm{GHz}$ Wi-Fi band for indoor. The energy levels confirmed the model described in Section II-A.

The chosen antennas were commercial antennas with $50\,\Omega$ impedance, an SMA connector and gains between 2 and $4\,\mathrm{dBi}$ for the target frequencies.

The matching networks were designed with Keysight Technologies' ADS 2020 software [27] (ADS), evaluating different topologies and adapting to a simulated impedance determined out of the available models of the next stages. The final topology adopted was a L-matching network due to its broader bandwidth. The final components values were obtained directly measuring with the vector network analyzer (VNA) E5063A from Keysight.

It is worth pointing out that the rectifier impedance depends on the input power due to the nonlinear characteristic of the diodes [19]. Consequently, the theoretical impedance was calculated assuming the target power levels (between -30 and $-15\,\mathrm{dBm}$) and for the two different paths after the rectification, described in the following Section III-C. In particular, the matching networks were designed without load for input 1 (i. e., as an open circuit after the rectification, favoring the charging process) and for input 2 with the equivalent impedance until the application block (favoring the cold-start, i. e., with no energy at all in the whole node).

B. Rectifier

Two analysis were made for the rectifier, relating to which diode and which rectification circuit to use.

1) Diode Selection: Besides the required low turn-on voltage and high switching speed mentioned in Section II-B that make Schottky diodes essential, in applications with high frequency and power restrictions, the junction capacitance and equivalent series resistance are critical for a good performance [28]. Hence, the importance of a good diode selection.

We tested several manufacturers with their Spice models and among them, we selected for further analysis Avago HSPS and HSMS series, Skyworks SMS7630, MACOM MA4E2502, Infineon BAT series, NXP BAT754, ST BAR42-43 and Panasonic DB27308. From which, the outstanding results were given by Infineon BAT63 and BAT15, Skyworks SMS7630 and Avago HSMS2850.

When working with high frequency the package parasitic elements become decisive. Thus, the chosen diode was Infineon BAT15 [29] as the one with by far the best performance including the package model for a series configuration, even when SMS7630 appeared beforehand as better. In this case, the simulation steps were made with ADS (see Figure 2) with a Greinacher circuit [17] and a matching network designed with large-signal s-parameter (LSSP) simulation in every case, optimizing between -30 and $-20\,\mathrm{dBm}$ of power input.

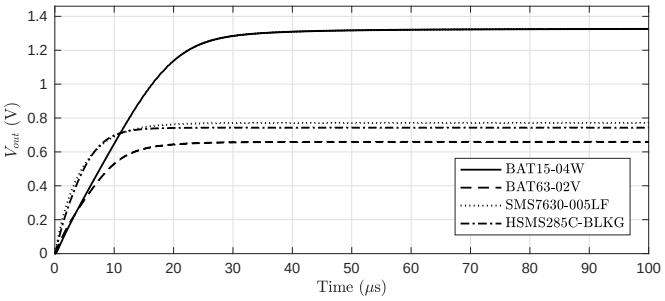

Fig. 2. Simulation of diodes performance in Greinacher configuration with package parasitic elements and impedance matching (ADS), showing V_{out} in time for $-20\,\mathrm{dBm}$ of input power with $100\,\mathrm{pF}$ capacitive load.

2) Circuit Selection: The rectifier purpose is not only the rectification of the input signal, but also a voltage boost. Each diode stage brings a higher voltage level, but on the other hand, it increases the losses by its power dissipation. Furthermore, the converter needs a minimum voltage to start operating and has as well a range with greater efficiency. Therefore, the circuit and its number of stages must be precisely designed for the expected conditions.

We analyzed the rectifying circuits of Greinacher, Cockcroft–Walton (both with 1, 2, 3 and 4 stages), Delon, diode bridge, peak detector, Greinacher quadrupler (full wave) and Dickson for RF (1 and 2 stages). From a first simulation with Spice (LTspice XVII [30]), the circuits of Cockcroft–Walton, Greinacher and Delon stood out. The next simulations were made with ADS, considering already the package parasitic elements of the diode BAT15-04W. A matching network was again designed for every case for the same conditions. A $100\,\mathrm{pF}$ capacitor was used as load instead of a bigger capacitor for faster simulation, since, due to the presence of the series capacitance of the diodes, its size has negligible effect. No resistive load was used as we supposed the next stage (*MSwitch*) in charging phase, i. e., with the switch open and isolated from the converter.

The simulation results (see Figure 3) threw that, for low input powers (e. g., at $-20\,\mathrm{dBm}$), Greinacher (1 stage) has the greatest efficiency (20%), while Delon the lowest (13%) and 2-stages Greinacher and Cockcroft–Walton similar ones halfway (16%). On the contrary, the last two circuits exhibit higher boost, as expected. The rest of versions with N-stages follow the trend, until the fourth stage in both circuits, where the voltage does not increase further for the target power. Although with the simplest Greinacher the voltage is already at valid levels, even for $-30\,\mathrm{dBm}$ as seen in Figure 3-b; we expected losses not reflected in the simulations dropping the output voltage. Consequently, we selected the Greinacher and Cockcroft–Walton circuits until the third stage for further study in the laboratory.

C. Store-and-Use Stage: "MSwitch"

The *MSwitch* stage is an innovative and autonomous dual-input circuit based on the store-and-use principle and on a

This article has been accepted for publication in a future issue of this journal, but has not been fully edited. Content may change prior to final publication. Citation information: DOI 10.1109/JIOT.2020.3024017, IEEE Internet of Things Journal

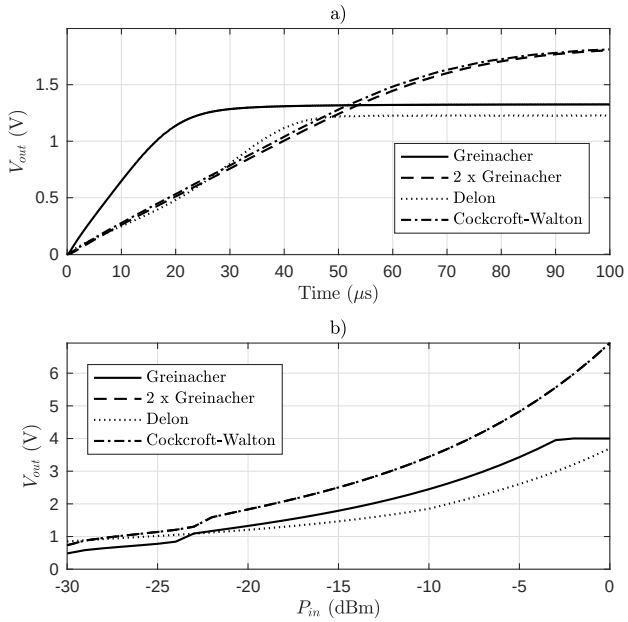

Fig. 3. Simulation of rectification circuits (ADS): (a) V_{out} in time at $-20\,\mathrm{dBm}$ (transient) and (b) V_{out} vs. the power input (HB). (2xGreinacher and Cockcroft-Walton overlap).

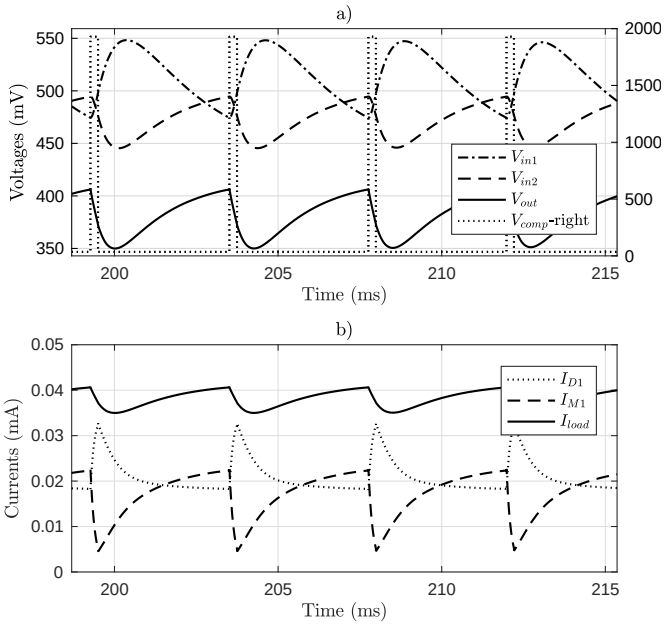

Fig. 5. *MSwitch Version 1*: Simulation of regular operation with Spice models. Cycles of input and output voltages (a) and currents (b). Dc input at every line of $45\,\mu\mathrm{W}$ at $700\,\mathrm{mV}$ open circuit. Load of $10\,\mathrm{k}\Omega$ and capacitors of $100\,\mathrm{nF}$.

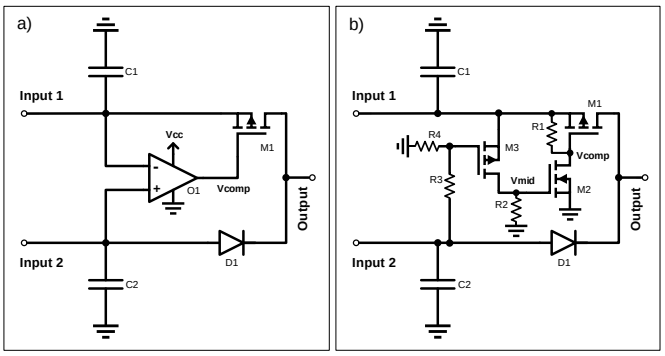

Fig. 4. Schematics of both versions of the store-and-use stage *MSwitch*: (a) with comparator (*Version 1*) and (b) with MOSFETs (*Version 2*).

switched capacitor design, capable of reducing the minimum average input power needed per RF band for an IoT application to operate.

MSwitch, in our two developed variants (see Figure 4), performs three functions: 1), it stores energy in time until the level is enough for running the electronics of the next stage (e. g., dc/dc converter) and for delivering it efficiently; 2), it mixes and regulates both input lines of the system in a dynamic manner, prioritizing the cold-start; and 3), it isolates the energy source from the load in order to not let the voltage drop, again being able to run the following electronics.

1) Working Principle: MSwitch adjusts the current delivery on both lines, being dragged largely from a line while the voltage remains higher than the other one, and even cutting it if the voltage drops, until the level rises again.

During the regular operation, power on both inputs is assumed and of around the same magnitude. *MSwitch Version 1* will perform a cycle where both inputs take turns to deliver energy (see Figure 5). The comparator (O1 in Figure 4) will switch on the transistor (M1) when the level of input 1 (V_{in1}) is above input 2 (plus some hysteresis) and, therefore, line 2 will be cut. As capacitor C1 discharges, C2 charges again and will eventually reach a higher level. Then, the comparator will switch off the transistor and the cycle will start again with the charge of C1. This process will not get corrupted over time decreasing the voltage level because of the comparator delay time, hysteresis and the proper election of the capacitors size.

For operating from cold-start, V_{cc} will be $0\,\mathrm{V}$ (it comes back from the converter stage, which is not charged yet), so V_{comp} will remain low as well by default. In this way, both lines conduct, self-adapting their currents through the diode until the dc/dc converter reaches a level where the comparator is able to operate (around $0.9\,\mathrm{V}$). Once this condition is satisfied, the store-and-use cycle starts, reaching lower power levels as described above.

In *Version 2*, the behavior of the comparator is replaced by two MOSFETs. We save its power consumption and dependence on the next stage, in exchange of giving up the hysteresis and using a voltage divider for adjusting V_{in2} in the comparison.

In this circuit, both lines auto-regulate their contribution at their best combination, maintaining an efficient voltage level and current flow. It achieves smoother changes, making easier the stabilization of the circuit without marked cycles and favoring the non-appearance of undesired voltage peaks. With Version 2, although the characteristic cycling of Version 1 appears only under special conditions of input power, the store-and-use principle still persists, since a line will only conduct when the voltage reaches a certain value. This means that under adverse energetic circumstances, a line would be cut as well, storing energy meanwhile.

Looking at both circuits from another perspective, *MSwitch*

This article has been accepted for publication in a future issue of this journal, but has not been fully edited. Content may change prior to final publication. Citation information: DOI 10.1109/JIOT.2020.3024017, IEEE Internet of Things Journal

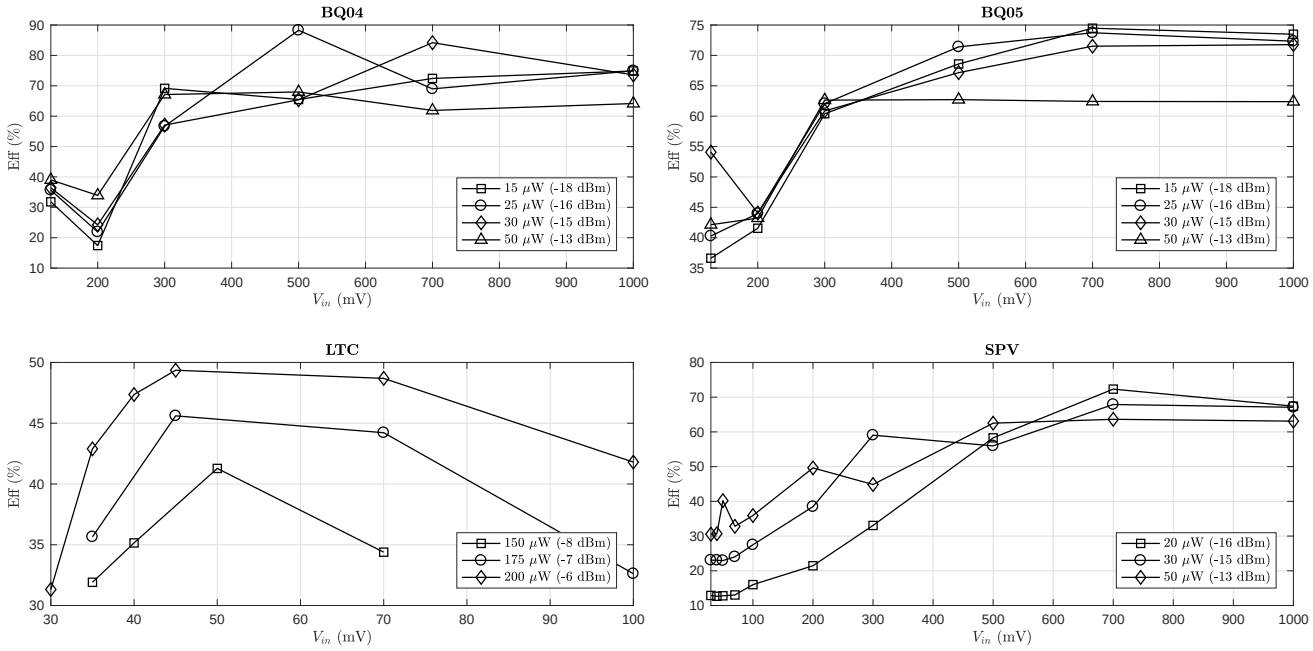

Fig. 6. Simulation of dc/dc converters efficiencies for different voltage and power inputs.

takes a variable voltage reference (input 2) for performing: in Version 1, a cyclic more-energetic burst operation; and in Version 2, an automatic adaption of the simultaneous delivered current. However, in our designs the voltage reference also delivers power. In addition, the fact that this reference is variable plays an important role for EH, since the voltage level depends on the ambient conditions and a fixed value would not be efficient.

Before the actual designs, we employed a P-channel MOSFET in depletion mode instead of the diode. This circuit was symmetrical and had a smoother cycle, as well as lower voltage barrier. These transistors are however not available on the market, so we opted for a Schottky diode without affecting significantly the operation.

D. DC/DC Converters Analysis

A study of the market options for ultra-low power made us focus on BQ25504, BQ25505, SPV1050 and LTC3108, after discarding BQ25570, MB39C831 and MCP1623 through a preliminary study of the features. We based our analysis first on the data-sheet information, carrying out afterward simulations with the available Spice models and the circuit designs recommended by the manufacturers. We went out of the specifications as needed while the model allowed it, and finally manufactured independent boards for their experimental characterization (see Section IV-C).

Figure 6 reports the results of simulations for a range of input voltages at different input powers, starting always from the lowest feasible in cold-start. The efficiency was calculated for an application period, from the triggering of the active mode to the recovery of the voltage using the converters flag. In the transient Spice simulations, we used a triggered load with two states, simulating sleep and active modes according to Section II-C. The configuration for the voltage output was always the closest to $3.3\,\mathrm{V}$ and MPPT was used when available.

The graphics in Figure 6 present BQ25504 [31] standing out with best efficiencies in general for a broad range of input powers, followed closely by BQ25505. LTC3108 and SPV1050 on the other side, cannot operate at low power inputs, although have a lower voltage level from where they can start running. In particular, LTC3108 reaches $30\,\mathrm{mV}$ at $-6\,\mathrm{dBm}$, although at that configuration it cannot work at voltages greater than the shown in the figure.

Due to the expected energy bursts as input of *MSwitch* Version 1, we also simulated this capability on the selected converters. The requirements are reduced to the ability of continuing their activity between pulses for the lower energy levels, avoiding to enter in the cold-start phase for each cycle (what would imply much lower efficiency). The simulations were successful for every converter at the target input powers for capacitances up to $140\,\mathrm{mF}$ (super-capacitor). This limit appeared as trade-off between, on one side, the losses of commercial super-capacitors and time of charging and, on the other side, the energy stored and delivered.

1) Load Energy Storage: The last energy storage element must be dimensioned according to the needs of the application. The energy of an application cycle must be encompassed in the capacitor within the voltage levels where the μC can operate, setting this the minimum capacitance. A too large one would be inefficient as well, since the charging time would substantially increase. Finally, we selected low leakage capacitors with the minimum value recommended by the converters data-sheets, since they sufficed for our application. For instance, in the case of the BQ25504, it meant 4.7 and $100\,\mu\mathrm{F}$ at the main and reserve outputs respectively.

This article has been accepted for publication in a future issue of this journal, but has not been fully edited. Content may change prior to final publication. Citation information: DOI 10.1109/JIOT.2020.3024017, IEEE Internet of Things Journal

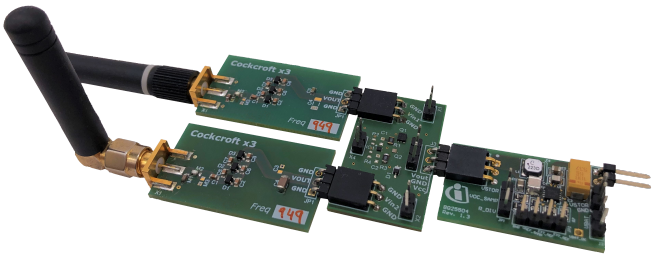

Fig. 7. Picture of the whole harvesting system (no application unit).

E. Application Stage

The chosen application unit for the IoT demonstrator was the Nordic nRF52 development kit [32]. This single board consists on an ARM Cortex M4 system on chip and a $2.4\,\mathrm{GHz}$ transceiver including the antenna. Most importantly, the theoretical power consumption according to the data-sheet is within the required range described in Section II-C.

The operation work-flow was developed to be duty-cycled as explained in Section II-C and the internal die temperature sensor was selected for the transmissions. A star topology was set, where the transmitted packets were received by another kit acting as gateway.

IV. Performance Analysis

With the best designs of every stage, we fabricated a prototype in standard FR4 technology for further analysis in the laboratory and demonstration purposes. Figure 7 depicts its modular fashion and dimensions with the circuits selected (see schematic in Figure S1). Following comes a performance analysis based on the measurements.

A. Impedance Matching and Rectification

Figure 8 presents the results of the manufactured rectifiers for $949\,\mathrm{MHz}$. We used only one frequency for simplicity of our designs. The open circuit voltage measurement was made with a signal generator N9310A from Keysight and an Agilent 34461A multimeter in high Z mode. The S_{11} parameter measurement was carried out with the output connected to V_{in2} and to BQ25504 in cold-start. We included the envelop detector circuit as reference, although it was not considered as a solution.

As expected, losses appear in contrast with the simulations, being the measured output voltage around 50% lower than the ideal scenario (see Figure 3-b). Although other factors also affect the result (including the measurement itself), the achieved S_{11} parameter influences highly the efficiency of the boards. Additionally and differing also from it, the circuits of 2xGreinacher and 2xCockcroft-Walton do not exactly overlap, having the last one a greater voltage.

This causes that, at least, a third stage must be used, since BQ25504 requires, according to the data-sheet, a minimum input of $600\,\mathrm{mV}$ for cold starting. Finally, we selected the circuit of 3xCockcroft-Walton, as its output voltage reaches the objectives (see Figure 8-a).

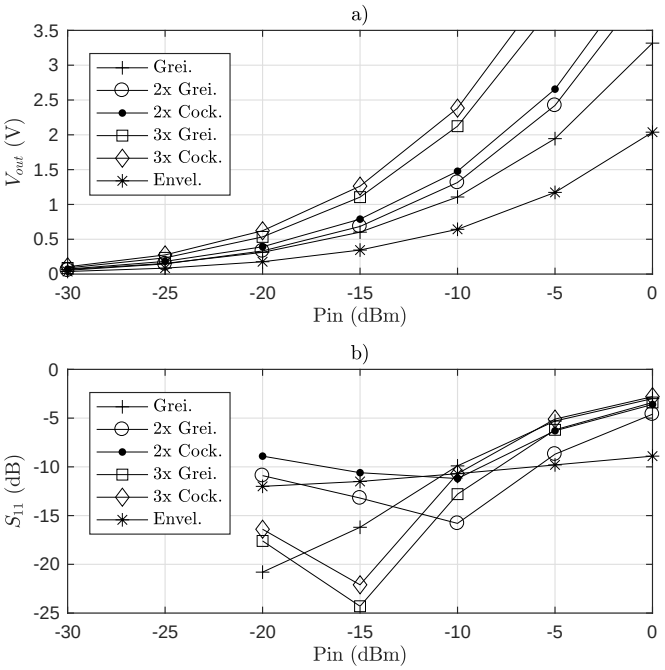

Fig. 8. Measurement of voltage output in open circuit (a) and S_{11} parameter with output connected to V_{in2} and to BQ25504 in cold-start (b) for the developed rectifiers at different power inputs and at a frequency of $949\,\mathrm{MHz}$.

B. MSwitch

We manufactured both versions of the circuit (Figure 4) and both worked as expected, presenting different features that make them interesting for different use-cases.

1) Version 1: It follows the behavior from the simulations (see Figure 5), with its marked cycles clearly seeing in Figure 9. It offers excellent performance for long-term store-and-use cycles in extremely low power scenarios, potentially charging a big capacitor and providing a powerful burst. Nevertheless, the need of a voltage source to run the comparator makes that the following stage must be able to stay powered on during these cycles or with only energy from input 2. Likewise, in more energy-favorable situations, the cycles can be shorter (meaning also smaller capacitors).

Notice that a big difference between the bands energy levels may cause that the voltage-drop in one line while conducting does not go below the other line, remaining this one always cut. In this case, although it is part of the casuistic, it may imply that the energy level on the conducting line is already enough for running the following electronics.

2) Version 2: It tends, on the other side, to the dual and simultaneous conduction over the pronounced cycles, as also expected from the simulations. Once a first dynamic voltage threshold is surpassed (with a powerful burst that helps the cold-start of the converter), the current on each line is self-adapted to the best conditions on the junction by the MOSFETs logic. Additionally, since there is no need of an external power source, the current delivery control initiates from the cold-start as well, increasing the efficiency and therefore the minimum harvested power.

It should be noticed in this version too, that due to the continuous dual conduction, a line would be very rarely

This article has been accepted for publication in a future issue of this journal, but has not been fully edited. Content may change prior to final publication. Citation information: DOI 10.1109/JIOT.2020.3024017, IEEE Internet of Things Journal

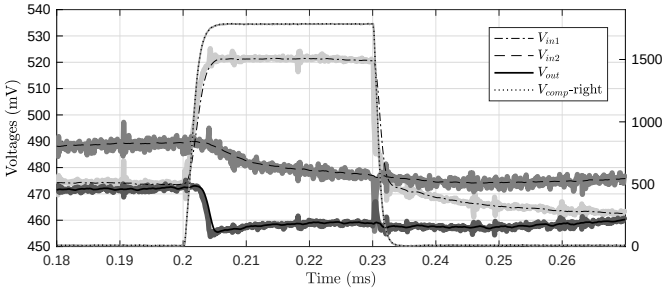

Fig. 9. Measurement of *MSwitch Version 1* cycle in time for an average of $110\,\mu\mathrm{W}$ and $10\,\mathrm{k}\Omega$ input power (dc) and impedance at both lines, with capacitors of $100\,\mathrm{nF}$. BQ25504 in cold-start used as load and V_{cc}. *Filtered data over shaded real measurements, for clearer view.*

completely cut. Only in case of sudden changes in the input or the load the MOSFETs logic would cut a line, avoiding a voltage-collapse and making it rise again, tending fast to the stabilization. This maintains high efficiency also in case of great difference in energy between the inputs or of a too power demanding load.

C. DC/DC Conversion

Our custom boards improved the performance of the converters evaluation kits. However, the measurements, as seen in Figure 10, reveal differences with the simulations of the Spice models (see Figure 6), where the minimum power for starting the operation from cold-start was higher in most of the cases.

The evaluation consisted of a first step where the converter was cold-started and brought to normal operation, measuring also the time needed (Table II). Next, with a variable load mimicking the application (as described in Section III-E), we measured the efficiency during an application cycle. For inputs too low for cold-starting, we brought the converter into operation and later decreased the input levels.

BQ25504 from Texas Instruments demonstrated as expected better response for ultra-low power conditions, counting with the best efficiencies and the lowest power inputs for cold-starting ($15\,\mu\mathrm{W}$ according to the data-sheet, although we measured $30\,\mu\mathrm{W}$). It needs, however, a minimum of $600\,\mathrm{mV}$ (as corrected in the data-sheet [31]) and it behaves at the input as a voltage source of $350\,\mathrm{mV}$, fixing the voltage until the MPPT is able to operate during normal charging process.

As also simulated in Section III-D, we characterized the timings of the converters with a $1\,\mathrm{mF}$ capacitor in every case (for equal conditions). Table II outlines, in the first column, the range of cold-start charging times for the power and voltage inputs measured in Figure 10 and with the application in sleep mode as load. The second and third columns detail the time that every converter is able to maintain adequate voltage levels for the µC with the application in active and sleep modes respectively, and no power input. Finally, the last column depicts the time able to remain out of the cold-start mode with the application in sleep mode and no power input. The results are consistent with the simulations, being every converter capable of operating in burst-mode with the tested conditions.

TABLE II
MEASUREMENT OF TIME CHARACTERIZATION OF DC/DC CONVERTERS

Converter	Charging Time (s)	Active Time (ms)	Sleep Time (s)	Alive Time (s)
BQ04	4160–42	54	237	242
BQ05	1551–69	114	202	706
LTC	16–2	33	355	871
SPV	843–66	118	431	636

D. IoT Application

The power measurements confirmed the awaited results. The energy consumption measured during the active mode was around $85\,\mu\mathrm{J}$; from which the transmission, set to the minimum, represented around $25\,\mu\mathrm{J}$. The deep-sleep power consumption was as well below the expected limit, around $300\,\mathrm{nA}$, although we decided to use a MOSFET as load-switch with the gate connected to the converters flag, in order to avoid boot problems at the cold-start.

V. WHOLE SYSTEM RESULTS

Once every stage was optimized, we tested the whole system with the innovative *MSwitch*. We also analyzed three more different approaches, alternatives to it for proper comparison: direct connection between rectifier and converter (single band), junction through two diodes with storing capacitors behind (exactly like input 2 of *MSwitch*) and in-series connection (as the design from Piñuela *et al.* [14]).

We carried out two experiments: 1), cold-start test, for finding the minimum input power with which can start operating and its efficiency throughout the whole input power range; and 2), hot operation test, for determining the minimum input power with which can maintain its operation, and its efficiency at a reference power level ($-15\,\mathrm{dBm}$). The efficiency was calculated, in the case of hot operation test, with the averaged application-cycle time (in a range between some seconds and a couple of minutes) and the known power consumption of the application active mode. In the the cold-start test, it was calculated with the time until the first packet was received and the energy needed to charge the capacitors of the dc/dc converter. For the setup, we used the previously mentioned signal generator and VNA, and for the in-series circuit, where two different grounds are required, we connected one of them to the grid through a transformer. In every case, the input power was equal at the two lines.

The results are summarized in Table III and Figure S2 and reveal how *MSwitch Version 2* responds better in every aspect analyzed. *MSwitch Version 1*, with similar performance as the in-series design, improves as well the single band and diode + capacitor cases. Comparing the absolute results of Table III with the literature results of Table I, we find a shift in both minimum input power and efficiencies. Since we tested as well under the same conditions the single-band and the in-series circuit [14] (that gives the best performance within the state-of-the-art) and in every case the operation was improved by *MSwitch*, we can therefore assure that this shift comes from a better implementation of the previous stages, in particular, the matching network and rectification. Besides, our system is

This article has been accepted for publication in a future issue of this journal, but has not been fully edited. Content may change prior to final publication. Citation information: DOI 10.1109/JIOT.2020.3024017, IEEE Internet of Things Journal

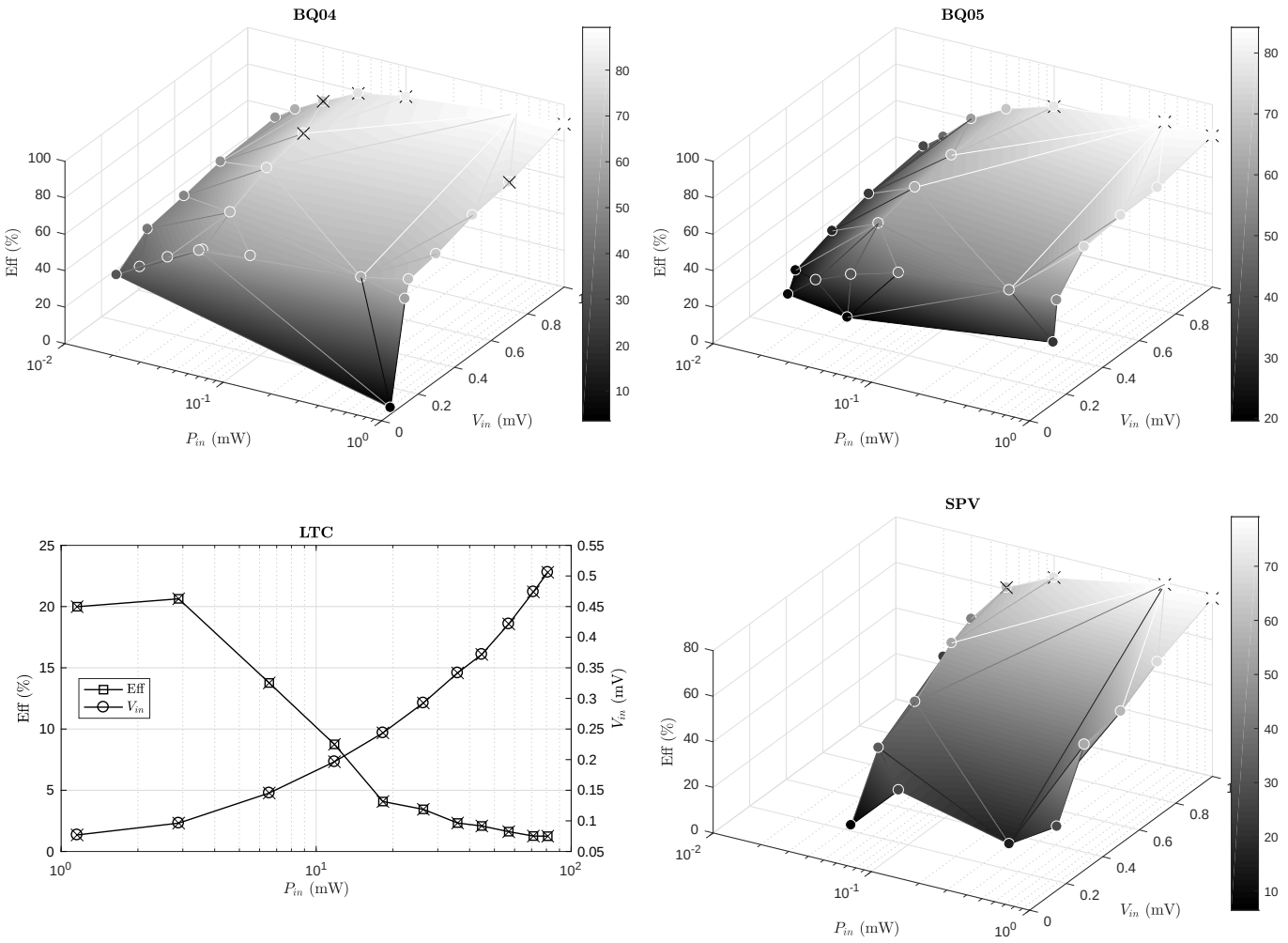

Fig. 10. Measurement of dc/dc converters efficiencies for different voltage and power inputs. Marked points (X) correspond to power-voltage input combinations able to cold-start.

the only one using a real IoT application, while most of the cases of Table III employ a resistor, or even a capacitive load, seeking for the best match to the output.

MSwitch Version 2 emerges with better performance in both cold-start and hot operations. It brings lower minimum input power for starting and maintaining its activity, and better efficiency. This turns into lower first-charge and cycle times for its IoT application. The lack of a component that needs a minimum voltage level for functioning (the comparator in Version 1) and its independent adaption of the currents per line (in contrast with the in-series circuit), make it perform at its best from the beginning and adapt quickly the contribution per line.

Besides, both *MSwitch* designs present an advantage over the in-series design, since its efficiency decreases extremely when one of the inputs is more powerful than the other. For instance, we applied an input of -12.5 and $-19.5\,\mathrm{dBm}$ at each line ($-15\,\mathrm{dBm}$ in average). The efficiency was improved by a 4.9 and 4.7% for Version 2 and 1 respectively, while it decreased by a 3% for the in-series circuit. It remained the same for the diode + capacitor design. In this situation, the current forced by the more powerful line makes collapse the voltage on the other input. This does not happen with the *MSwitch* auto-regulation, since it takes advantage of the powerful source without collapsing the second one.

VI. Conclusion

In this work, we have introduced an innovative RFEH dual-band design for energy-autonomous IoT nodes, that improves the current state-of-the-art in numerous perspectives. The circuits, in two different versions, were tested and demonstrated within a complete developed system including rectification, dc/dc conversion and a final IoT application.

We analyzed likewise with several simulations and measurements the whole spectrum of dc/dc converters in the market, characterizing their responses for ultra-low power conditions, often out of the data-sheet descriptions. BQ25504 from Texas Instruments appeared as the best candidate, reaching the lowest input power levels and implementing MPPT, although fixing its input at $350\,\mathrm{mV}$ during its cold-start.

Furthermore, we carried out a deep analysis of the commercially available diodes and state-of-the-art rectification schemes, selecting Infineon BAT15, due to the package parasitic elements; and Greinacher and Cockcroft-Walton circuits

This article has been accepted for publication in a future issue of this journal, but has not been fully edited. Content may change prior to final publication. Citation information: DOI 10.1109/JIOT.2020.3024017, IEEE Internet of Things Journal

TABLE III
PERFORMANCE OF MSWITCH SYSTEMS IN COMPARISON WITH OTHER SOLUTIONS AND SINGLE BAND

Technology	**Frequency**	**Minimum RF P_{in} @ Output Voltage ***			**Conversion Efficiency @ RF P_{in} ***	
MSwitch v1 BAT15 Schottky	949 MHz	Cold-start	$-15.0\,\mathrm{dBm}$ (IoT app)	+11%	13.1% @ $-15\,\mathrm{dBm}$ (end-to-end, lab., hot oper.)	+9.2%
		Hot Oper.	$-16.6\,\mathrm{dBm}$ (IoT app)	+29%		
MSwitch v2 BAT15 Schottky	949 MHz	Cold-start	$-16.3\,\mathrm{dBm}$ (IoT app)	+34%	13.3% @ $-15\,\mathrm{dBm}$ (end-to-end, lab., hot oper.)	+9.5%
		Hot Oper.	$-16.8\,\mathrm{dBm}$ (IoT app)	+31%		
Single band BAT15 Schottky	949 MHz	Cold-start	$-14.5\,\mathrm{dBm}$ (IoT app)	-	3.7% @ $-15\,\mathrm{dBm}$ (end-to-end, lab., hot oper.)	-
		Hot Oper.	$-15.1\,\mathrm{dBm}$ (IoT app)	-		
Diode + cap. / line BAT15 Schottky	949 MHz	Cold-start	$-15.6\,\mathrm{dBm}$ (IoT app)	+22%	5.9% @ $-15\,\mathrm{dBm}$ (end-to-end, lab., hot oper.)	+2.1%
		Hot Oper.	$-15.8\,\mathrm{dBm}$ (IoT app)	+15%		
In-series [14] BAT15 Schottky	949 MHz	Cold-start	$-15.1\,\mathrm{dBm}$ (IoT app)	+13%	10.2% @ $-15\,\mathrm{dBm}$ (end-to-end, lab., hot oper.)	+6.4%
		Hot Oper.	$-16.6\,\mathrm{dBm}$ (IoT app)	+29%		

**Last sub-column compares the result over the single band option.*

(up to a third level), in spite of the quality of the matching network influencing severely their performances.

The whole system presented finally an improvement over the single band case of a 34 and 31% in the minimum RF power input for the cold-start and hot operation respectively, and of a 9.5% in the efficiency at $-15\,\mathrm{dBm}$ (value taken as reference). Moreover, while *MSwitch Version 1* exhibits similar results as the in-series design (the best performing circuit up to the date to the eyes of the authors [14]); *Version 2* improves by a 21 and 2% its minimum RF power input for the cold-start and hot operation respectively, and by a 3.1% its efficiency (see Table III). Besides, when the inputs have different power levels, both versions of *MSwitch* even increase their efficiencies, while the operation of the rest of the circuits get compromised. We encountered nonetheless an offset of the absolute values in our experiments in relation to the literature. We attribute it to a better implementation of the impedance matching and rectification stages and to the use of a real IoT application, since, under the same conditions, both in-series circuit and single-band exhibited lower performance than *MSwitch*, as described above.

In conclusion, we demonstrated how *MSwitch* is able to operate with off-the-shelf dc/dc converters under ultra-low power conditions and in real dynamic environments, where the band levels do not have to be equal or constant; with RFEH or any other harvesting method, mixing in an efficient manner two power lines.

ACKNOWLEDGMENT

This work was partially supported by the ECSEL Joint Undertaking through the Electronic Component Systems for European Leadership Joint Undertaking under grant agreement No 737434. This Joint Undertaking receives support from the German Federal Ministry of Education and Research and the European Union's Horizon 2020 research and innovation program and Slovakia, Netherlands, Spain, Italy.

REFERENCES

[1] G. Zhou, L. Huang, W. Li, and Z. Zhu, "Harvesting ambient environmental energy for wireless sensor networks: a survey," *Journal of Sensors*, vol. 2014, pp. 1–20, 2014.

[2] P. Kamalinejad, C. Mahapatra, Z. Sheng, S. Mirabbasi, V. C. Leung, and Y. L. Guan, "Wireless energy harvesting for the internet of things," *IEEE Communications Magazine*, vol. 53, no. 6, pp. 102–108, 2015.

[3] H. Jayakumar, K. Lee, W. S. Lee, A. Raha, Y. Kim, and V. Raghunathan, "Powering the internet of things," in *Proceedings of the 2014 international symposium on Low power electronics and design*. ACM, 2014, pp. 375–380.

[4] F. Moreno-Cruz, A. Escobar-Molero, E. Castillo, M. Becherer, A. Rivadeneyra, and D. P. Morales, "Why use rf energy harvesting in smart grids," in *2018 IEEE 23rd International Workshop on Computer Aided Modeling and Design of Communication Links and Networks (CAMAD)*. IEEE, 2018, pp. 1–6.

[5] X. Lu, P. Wang, D. Niyato, D. I. Kim, and Z. Han, "Wireless networks with rf energy harvesting: A contemporary survey," *IEEE Communications Surveys & Tutorials*, vol. 17, no. 2, pp. 757–789, 2015.

[6] F. Moreno-Cruz, V. Toral López, F. J. Romero, C. Hambeck, D. P. Morales, and A. Rivadeneyra, "Use of low-cost printed sensors with rf energy harvesting for iot," in *2019 Smart Systems Integration (SSI)*, 2019.

[7] G. Singh, R. Ponnaganti, T. Prabhakar, and K. Vinoy, "A tuned rectifier for rf energy harvesting from ambient radiations," *AEU-International Journal of Electronics and Communications*, vol. 67, no. 7, pp. 564–569, 2013.

[8] S. S. Chouhan, M. Nurmi, and K. Halonen, "Efficiency enhanced voltage multiplier circuit for rf energy harvesting," *Microelectronics Journal*, vol. 48, pp. 95–102, 2016.

[9] Powercast Co., "Power harvester development kit," http://www.powercastco.com/products/development-kits/#P2110-EVB, accessed: 26-04-2019.

[10] S. Agrawal, S. K. Pandey, J. Singh, and M. S. Parihar, "Realization of efficient rf energy harvesting circuits employing different matching technique," in *Fifteenth International Symposium on Quality Electronic Design*. IEEE, 2014, pp. 754–761.

[11] S. Oh and D. D. Wentzloff, "A- 32dbm sensitivity rf power harvester in 130nm cmos," in *2012 IEEE radio frequency integrated circuits symposium*. IEEE, 2012, pp. 483–486.

[12] M. Stoopman, S. Keyrouz, H. J. Visser, K. Philips, and W. A. Serdijn, "Co-design of a cmos rectifier and small loop antenna for highly sensitive rf energy harvesters," *IEEE Journal of Solid-State Circuits*, vol. 49, no. 3, pp. 622–634, 2014.

[13] B. R. Franciscatto, V. Freitas, J.-M. Duchamp, C. Defay, and T. P. Vuong, "High-efficiency rectifier circuit at 2.45 ghz for low-input-power rf energy harvesting," in *2013 European Microwave Conference*. IEEE, 2013, pp. 507–510.

[14] M. Piñuela, P. D. Mitcheson, and S. Lucyszyn, "Ambient rf energy harvesting in urban and semi-urban environments," *IEEE Transactions on microwave theory and techniques*, vol. 61, no. 7, pp. 2715–2726, 2013.

[15] T.-L. Nguyen, Y. Sato, and K. Ishibashi, "A 2.77 μw ambient rf energy harvesting using dtmos cross-coupled rectifier on 65 nm sotb and wide bandwidth system design," *Electronics*, vol. 8, no. 10, p. 1173, 2019.

[16] P. Xu, D. Flandre, and D. Bol, "Analysis, modeling, and design of a 2.45-ghz rf energy harvester for swipt iot smart sensors," *IEEE Journal of Solid-State Circuits*, vol. 54, no. 10, pp. 2717–2729, 2019.

[17] J. Park, Y. Kim, Y. J. Yoon, J. So, and J. Shin, "Rectifier design using distributed greinacher voltage multiplier for high frequency wireless power transmission," *Journal of electromagnetic engineering and science*, vol. 14, no. 1, pp. 25–30, 2014.

[18] M. B. Asl and M. H. Zarifi, "RF to DC micro-converter in standard CMOS process for on-chip power harvesting applications," *AEU - International Journal of Electronics and Communications*, vol. 68, no. 12, pp. 1180–1184, dec 2014.

[19] U. Muncuk, K. Alemdar, J. D. Sarode, and K. R. Chowdhury, "Multi-band ambient rf energy harvesting circuit design for enabling batteryless sensors and iot," *IEEE Internet of Things Journal*, vol. 5, no. 4, pp. 2700–2714, 2018.

[20] E. Khansalee, K. Nuanyai, and Y. Zhao, "A dual-band rectifier for RF energy harvesting," *Engineering Journal*, vol. 19, no. 5, pp. 189–197, oct 2015.

[21] D. D. Donno, L. Catarinucci, and L. Tarricone, "An UHF RFID energy-harvesting system enhanced by a DC-DC charge pump in silicon-on-insulator technology," *IEEE Microwave and Wireless Components Letters*, vol. 23, no. 6, pp. 315–317, jun 2013.

[22] X. Liu and E. Sánchez-Sinencio, "A highly efficient ultralow photovoltaic power harvesting system with mppt for internet of things smart nodes," *IEEE transactions on very large scale integration (vlsi) systems*, vol. 23, no. 12, pp. 3065–3075, 2015.

[23] M. Russo, P. Šolić, and M. Stella, "Probabilistic modeling of harvested gsm energy and its application in extending uhf rfid tags reading range," *Journal of Electromagnetic Waves and Applications*, vol. 27, no. 4, pp. 473–484, 2013.

[24] A. Palaios, V. Miteva, J. Riihijärvi, and P. Mähönen, "When the whispers become noise: A contemporary look at radio noise levels," in *Wireless Communications and Networking Conference (WCNC), 2016 IEEE*. IEEE, 2016, pp. 1–7.

[25] M. Yılmaz, D. G. Kuntalp, and A. Fidan, "Determination of spectrum utilization profiles for 30 mhz–3 ghz frequency band," in *Communications (COMM), 2016 International Conference on*. IEEE, 2016, pp. 499–502.

[26] Electronic Communications Committee (ECC) within the European Conference of Postal and T. A. (CEPT), "The european table of frequency allocations and applications in the frequency range 8.3 khz to 3000 ghz (eca table)," 2016.

[27] Keysight Technologies, "Advanced design system (ADS) 2020," Sep. 2019.

[28] D. Pavone, A. Buonanno, M. D'Urso, and F. Della Corte, "Design considerations for radio frequency energy harvesting devices," *Progress In Electromagnetics Research B*, vol. 45, pp. 19–35, 2012.

[29] Infineon Technologies, *Series silicon RF Schottky diode pair. BAT15-04W datasheet*, Jun. 2018.

[30] Linear Technologies, "Ltspice XVII," Apr. 2020.

[31] Texas Instruments, *Ultra Low-Power Boost Converter With Battery Management For Energy Harvester Applications. BQ25504 datasheet*, Oct. 2011, revised Nov. 2019.

[32] Nordic Semiconductor, *nRF52 DK for Bluetooth LE, Bluetooth mesh, ANT and 2.4 GHz applications. nRF52 product brief*, Apr. 2019.